

Magnetic resonance relaxation time in evaluating the cyst fluid characteristics of endometrioma

Kentaro Takahashi^{1,3}, Saori Okada¹,
Masako Okada¹, Manabu Kitao¹, Yasushi Kaji²
and Kazuro Sugimura²

Departments of ¹Obstetrics and Gynecology and ²Radiology,
Shimane Medical University, 89-1 Enya-cho, Izumo 693, Japan

³To whom correspondence should be addressed

To determine whether the cyst fluid characteristics of endometrioma can be evaluated by magnetic resonance imaging (MRI), 36 endometriomas obtained from 24 patients (age range 21–43 years; mean 34 years) were studied. MRI was performed <2 weeks before laparoscopy or laparotomy. Comparative studies of the density and concentration of iron in the endometrioma and the signal intensity (SI) of MRI [calculated relaxation time T_1 value, calculated relaxation time T_2 value, signal intensity on a T_1 -weighted image (T_1 SI) and on a T_2 -weighted image (T_2 SI) of the cyst; T_1 SI/signal intensity of the gluteus maximus muscle (MSI), and T_2 SI/MSI of the cyst] were performed. The density of the cyst fluid and its iron concentration were found to be directly proportional. There was a significant relationship between the concentration of iron and the T_2 SI, T_2 SI/MSI and calculated T_2 values. In particular, the concentration of iron and the ratio of T_2 SI/MSI were inversely proportional. Therefore, T_2 SI/MSI reflected the concentration of iron in endometriomas without recourse to measurement of the calculated T_2 value, which suggests that the MRI and T_2 signal intensity may be useful for evaluating the cyst fluid characteristics of endometriomas.

Key words: endometrioma/iron concentration/magnetic resonance imaging/relaxation time

Introduction

Endometriomas, the so-called chocolate cysts of the ovary, are common in patients with advanced endometriosis. Surgical resection has been the main treatment. Recently, ultrasound-guided aspiration of the endometrioma has been proposed as one step in a therapeutic approach (Aboulghar *et al.*, 1991; Abu-Musa *et al.*, 1991; Vercellini *et al.*, 1992; Aisa *et al.*, 1994).

The cyst fluid characteristics of the endometrioma must be determined prior to puncture as it is difficult to aspirate an advanced or chronic endometrioma. A non-invasive evaluation of the cyst fluid would allow the determination of the stage of development, and then selection of treatment. However, conventional imaging techniques such as computed tomography and ultrasonography cannot be used in evaluating the

cyst fluid. Magnetic resonance imaging (MRI) is useful in diagnosing endometriosis (Nishimura *et al.*, 1987; Arrive *et al.*, 1989; Zawin *et al.*, 1989; Takahashi *et al.*, 1994), although endometriomas are sometimes indistinguishable from other haemorrhagic adnexal lesions (Outwater *et al.*, 1993). An endometrioma is formed by repeated haemorrhage. The cyst fluid can show a varying content of haemoglobin. In addition, the fluid can change as the cyst progresses; the concentration of iron can increase exponentially and the viscosity of the fluid can rise. Therefore we investigated the relationship between the magnetic resonance relaxation time of surgically proven endometrioma and the concentration of iron in cyst fluid.

Materials and methods

We evaluated 36 endometriomas from 24 Japanese patients (aged 21–43 years; mean 34 years) who were due to have surgery (laparoscopy or laparotomy). In every patient, surgery was performed within 2 weeks of MRI and before the next menstruation. Cyst fluid was collected post-cystectomy by laparotomy or, when a laparoscopic cystectomy was performed, fluid was aspirated intra-operatively, taking care to exclude blood or exudate. The density and concentration of iron in the cyst fluid were measured by the Gay–Lussac-type specific gravity bottle (Aoi Manufactory Inc., Tokyo, Japan) and the 2-nitroso-5-(*N*-propyl-*N*-sulphopropylamino) phenol method (Saito *et al.*, 1981) with an Fe C-test Wako (Wako Pure Chemical Industries Ltd, Osaka, Japan) respectively.

MRI was performed with a 1.5-T superconducting unit (Signa; GE Medical Systems, Milwaukee, WI, USA). A spin-echo multisection imaging technique was used in all examinations. Relaxation time T_1 -weighted [spin-echo 600/15 ms (repetition time/echo time)], proton density (2200/15 ms) and relaxation time T_2 -weighted (2200/80 ms) axial images were obtained with a body coil in all patients. Data acquisition was performed twice. Two signals were averaged on both T_1 - and T_2 -weighted imaging. The field of view was 32×32 cm and the slice thickness was 6 mm with a 2 mm interslice gap. A 256×256 matrix was used for T_1 -weighted imaging and a 256×192 matrix for T_2 -weighted imaging. Inferior and superior saturation pulses were applied in all the sequences. Gradient moment nulling or respiratory compensation were not used.

The approximate relationship between image intensity and tissue and imager parameters in spin-echo imaging can be described by the following formula:

$$I = N(H)f(v) \cdot \exp(-T_E/T_2) \times [1 - \exp(-T_R/T_1)],$$

where I is the image intensity, $N(H)$ is the hydrogen density, $f(v)$ is the velocity effect, T_E is the delay between radio frequency excitation and the spin-echo, T_R is the interval between excitations, and T_1 and T_2 are the tissue relaxation times. A calculated T_1 image was obtained with the T_1 -weighted and the proton density images. For the calculation of T_1 values, manual prescanning was performed to maintain the

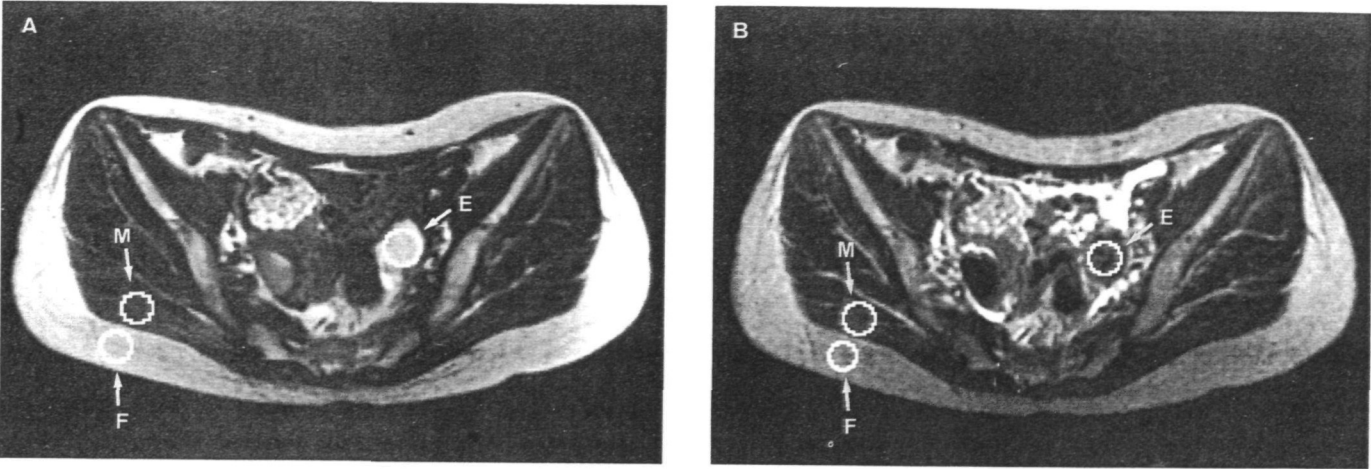


Figure 1. Magnetic resonance image of the left endometrial cyst. (A) T_1 -weighted image [spin-echo sequence, repetition time (T_R) 600 ms, echo time (T_E) 15 ms] and operator-defined regions of interest (E = endometrial cyst; M = muscle; F = fat) are shown. (B) T_2 -weighted image (spin-echo sequence, T_R 2200 ms, T_E 80 ms) and operator-defined regions of interest (E, M and F) are shown. The endometrial cyst demonstrates a high signal intensity on the T_1 -weighted image and a low signal intensity on the T_2 -weighted image.

same gain as for recording values. A calculated T_2 image was obtained with the T_2 -weighted and the proton density images. We designated a region of interest on the T_1 -weighted and T_2 -weighted images covering the endometrial cyst as widely as possible. A region of interest >100 pixels was drawn in the gluteus maximus. We designated the same region of interest in the endometrial cyst on the calculated images (Figure 1). Most endometrial cysts are a little heterogeneous. Therefore, the signal intensity (SI) on each conventional image was measured three times; the T_1 and T_2 values on each calculated image were measured three times, and the average calculated. Intra-observer variability was $\leq 0.8\%$ of the calculated T_1 value, and $\leq 1.1\%$ of the calculated T_2 value. We obtained the calculated T_1 value, calculated T_2 value and the signal intensities on the T_1 -weighted image (T_1 SI) and on the T_2 -weighted image (T_2 SI) of each endometrial cyst. To normalize the T_1 SI and T_2 SI values among the subjects, we calculated the ratios of signal intensity of the endometrial cyst/the signal intensity of the gluteus maximus muscle on the T_1 -weighted image (T_1 SI/MSI), as well as the signal intensity of the endometrial cyst/the signal intensity of the gluteus maximus muscle on the T_2 -weighted image (T_2 SI/MSI). The concentration of iron and the signal intensity of each image were compared statistically using a χ^2 analysis. A probability of $<5\%$ was accepted as statistically significant.

Results

Figure 2 shows a significant positive correlation between the concentration of iron and the density of the fluid in the endometriomas ($r = 0.847$, $P = 0.0001$). Table I shows the correlations between the concentration of iron and the signal intensity of each image. There was no significant correlation between the iron concentration and the calculated T_1 value or its associated signal intensity ratios. However, there was a significant correlation between the iron concentration and the calculated T_2 value, T_2 SI and T_2 SI/MSI. The coefficients of correlation between the iron concentration and the 1/calculated T_2 value, the value of T_2 SI and the ratio of T_2 SI/MSI were 0.612 ($P = 0.0001$), -0.684 ($P = 0.0001$) and -0.856 ($P = 0.0001$) respectively (Figures 3–5). The concentration of iron was strongly negatively correlated with T_2 SI/MSI, which suggested an inverse relationship between these two factors.

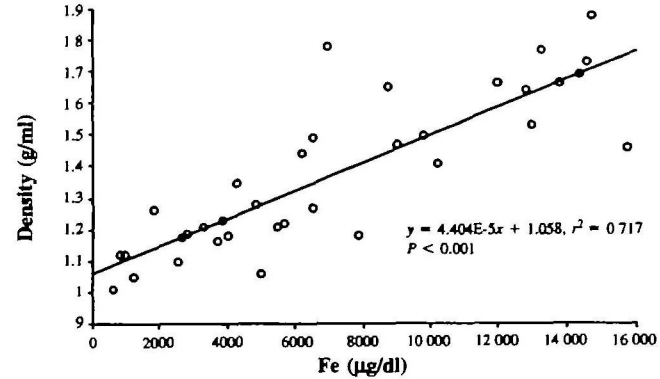


Figure 2. Positive correlation between the iron concentration and the density of the endometrioma.

Table I. Correlations between the iron concentration and signal intensity (SI) of each image

	r^2	P value
Calculated T_1 value	9.221×10^{-6}	0.9893
T_1 SI ^a	4.660×10^{-5}	0.9753
T_1 SI/MSI ^b	0.011	0.6281
Calculated T_2 value	0.432	0.0001
T_2 SI ^c	0.467	0.0001
T_2 SI/MSI ^d	0.732	0.0001

^aSignal intensity on T_1 -weighted image of endometrial cyst.
^bSignal intensity of endometrial cyst/signal intensity of gluteus maximus muscle on T_1 -weighted image.
^cSignal intensity on T_2 -weighted image of endometrial cyst.
^dSignal intensity of endometrial cyst/signal intensity of gluteus maximus muscle on T_2 -weighted image.

Discussion

An endometrioma is a haemorrhagic cyst whose appearance on MRI varies over time. An acute haematoma shows hypointensity on both T_1 - and T_2 -weighted images, which is consistent with the present of deoxyhaemoglobin. A subacute haematoma is seen as isointense fat on the T_1 -weighted image,

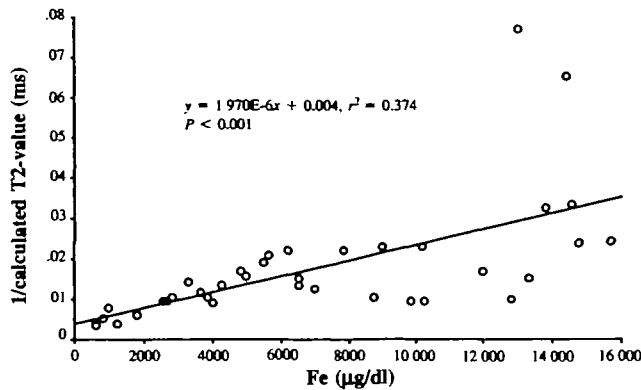


Figure 3. Inverse correlation between the iron concentration and the calculated T_2 value of the endometrioma.

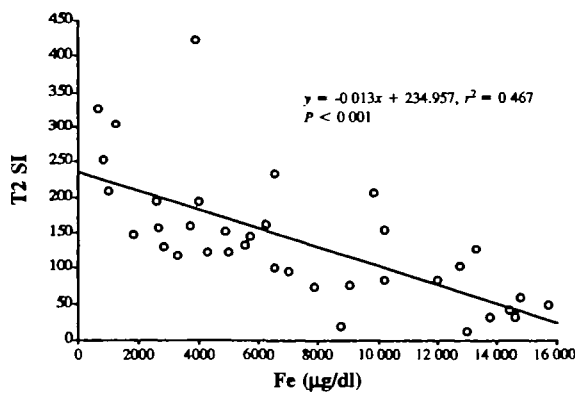


Figure 4. Negative correlation between the iron concentration and the T_2 signal intensity (SI) of the endometrioma.

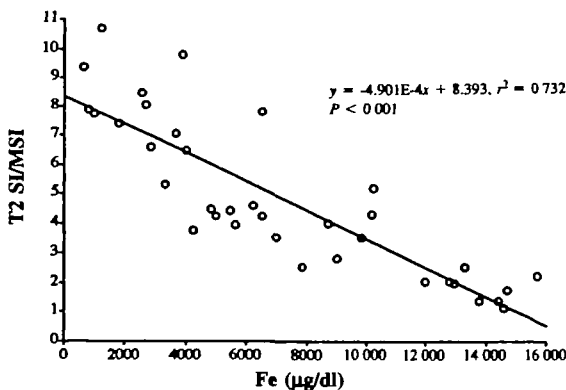


Figure 5. Negative correlation between the iron concentration and the ratio of the T_2 signal intensity (SI) of the endometrioma/the signal intensity of the gluteus maximus muscle (MSI) on a T_2 -weighted image.

and appears as iso- or hyperintense relative to urine on the T_1 -weighted image, consistent with the concentration of free methaemoglobin. Endometriomas undergo cyclic bleeding over the years. The fresh blood that results from repeated bleeding mixes with the pre-existing aged blood. Togashi *et al.* (1991) suspected that a high viscosity of the cyst content, as is characteristic of the endometrial cyst, contributes to the mechanism of shading. An endometrioma diagnosed by MRI shows

a variable intensity on T_2 -weighted images because of cyst content.

In our experience, the cyst fluid characteristics influence the management of endometriomas, and the aspiration of advanced or chronic endometriomas is more difficult. Therefore, it is clinically important to evaluate the cyst fluid characteristics of an endometrioma prior to aspiration. The purpose of this study was to evaluate the relationship between the cyst concentration of iron and the signal intensity on MRI. We focused on the content of the endometrioma in that a change in its content may be associated with its age. Previous reports (Bradley and Schmidt, 1985; Stark *et al.*, 1985) on subarachnoid haemorrhages stated that their appearance on MRI is related variously to the presence of methaemoglobin, free Fe^{3+} ions, haematocrit, protein and lipids. In particular, the concentration of methaemoglobin and of free Fe^{3+} ions is related to the T_2 value, while the haematocrit is related to the T_1 value. The endometrial cyst differs from intracranial haematomas in that the cyst content shows a marked increase in the concentration of iron and in viscosity with time because of the degradation of old blood.

For the relationship between the cyst concentration of iron and the MRI measurements, T_1 and T_2 are the most important values. However, it is very complicated to obtain these values. To obtain the T_2 value, a calculated T_2 image must be obtained with a T_2 -weighted image and a proton density image. We have to perform manual prescanning to maintain the values. Additional time and complicated work is required for these procedures. On the other hand, it is easy to obtain $T_1\text{SI}$ and $T_2\text{SI}$ values. The procedure only involves setting a region of interest. If $T_1\text{SI}$ and $T_2\text{SI}$ are reliable measurements, then this method may be useful in routine work. We used a two-points technique to obtain the relaxation time. We understand that the two-points technique has certain limitation. However, this technique is clinically useful because no additional scanning is necessary. In this study, a very accurate relaxation time is not required. Therefore, we think that the relaxation time obtained by this two-points technique is acceptable. If a correlation with iron concentration is expected, it might be necessary to perform gradient echo measurements to ensure that the shortening in T_2 is caused by iron and not viscosity. However, gradient echo measurements are very sensitive to the iron concentration, which is usually extremely high. When gradient echo is used, an echo signal cannot be obtained from most endometrial cysts, and thus we cannot observe a signal difference between different lesions. For these reasons we used spin-echo sequences.

Our study revealed that the calculated T_2 value and the concentration of iron were negatively correlated, which indicates that fewer factors influence the relaxation time for an endometrioma than for an intracranial haematoma, as found by Bradley and Schmidt (1985). Our results agree with those that Fullerton (1988) observed, i.e. a corresponding decrease in the relaxation time with an increase in the concentration of iron and the viscosity of the cyst fluid, although this study indirectly addressed the question of a correlation between iron content and viscosity by determining the density instead of the viscosity. The viscosity and protein concentration of a fluid

are known to influence its signal intensity (Fullerton, 1988). In our study we did not measure the protein concentration in addition to the density, because the iron concentration we found reflects the protein concentration. The density and concentration of the endometrial cyst fluid were directly proportional. Because an endometrioma is a retention cyst, we suspect that its water content decreases with time, while the level of protein and minerals increases. We specifically evaluated the iron concentration, the mineral in the endometrioma. Many factors may affect the T_2 relaxation time. We only evaluated the relationship between the relaxation time and the iron concentration. It seems that the relationship between iron concentration and T_2 SI/MSI may be better than that between the iron concentration and the T_2 relaxation time.

Because the T_2 SI/MSI ratio reflects the iron concentration of the endometrioma without recourse to the measurement of the calculated T_2 value, this parameter may be useful for evaluating the progression of the cyst. Although the final conclusion must be evaluated in a prospective study which includes a large series of endometriomas, we recommend that an endometrioma should be evaluated by MRI prior to aspiration. Naturally these findings should only be used in conjunction with other results to determine the feasibility of cyst aspiration.

References

- Aboughar, M.A., Mansour, R.T., Serour, G.I. and Rizk, B. (1991) Ultrasonic transvaginal aspiration of endometriotic cysts: an optional line of treatment in selected cases of endometriosis. *Hum. Reprod.*, **6**, 1408–1410.
- Abu-Musa, A., Takahashi, K., Nagata, H. and Kitao, M. (1991) Pregnancy following transvaginal sonographic guided aspiration of endometrioma. *Gynecol. Obstet. Invest.*, **31**, 90–92.
- Aisa, F., Diaz, M. and Leal, C. (1994) Experience with transvaginal ultrasound-guided aspiration of cystic ovarian masses. *Hum. Reprod.*, **9** (Suppl. 4), 211.
- Arrive, L., Hircal, H. and Martine, M.C. (1989) Pelvic endometriosis: MR imaging. *Radiology*, **171**, 687–692.
- Bradley, W.G. and Schmidt, P.G. (1985) Effect of methemoglobin formation on the MR appearance of subarachnoid hemorrhage. *Radiology*, **156**, 99–103.
- Fullerton, G.D. (1988) Physiologic basis of magnetic relaxation. In Stark, D.D. and Bradley, W.G. (eds), *Magnetic Resonance Imaging*. 2nd edn, Mosby, Philadelphia, PA, USA, pp. 36–55.
- Nishimura, K., Togashi, K., Itoh, K. *et al.* (1987) Endometrial cysts of the ovary; MR imaging. *Radiology*, **162**, 315–318.
- Outwater, E., Schiebler, M.L., Owen, R.S. and Schnall, M.D. (1993) Characterization of hemorrhagic adnexal lesions with MR imaging: blinded reader study. *Radiology*, **186**, 489–494.
- Saito, M., Horiguchi, D. and Kina, K. (1981) Spectrophotometric determination of traces of iron (II) with novel water-soluble nitrosophenol derivatives. *Bunseki Kagaku*, **30**, 635–639.
- Stark, D.D., Moseley, M.E., Bacon, B.R. *et al.* (1985) Magnetic resonance imaging and spectroscopy of hepatic iron overload. *Radiology*, **154**, 137–142.
- Takahashi, K., Okada, S., Ozaki, T. *et al.* (1994) Diagnosis of pelvic endometriosis by magnetic resonance imaging using 'fat-saturation' technique. *Fertil. Steril.*, **62**, 973–977.
- Togashi, K., Nishimura, K., Kimura, I. *et al.* (1991) Endometrial cysts: diagnosis with MR imaging. *Radiology*, **180**, 73–78.
- Vercellini, P., Vendola, N., Bocciolone, L. *et al.* (1992) Laparoscopic aspiration of ovarian endometriomas. Effect with postoperative gonadotropin releasing hormone agonist treatment. *J. Reprod. Med.*, **37**, 577–580.
- Zawin, M., McCarthy, S.M., Scott, L. and Comite, F. (1989) Endometriosis: appearance and detection at MR imaging. *Radiology*, **171**, 693–696.

Received on September 1, 1995; accepted on February 2, 1996